Electrization of the Quartz Glass Surface by Electron Beams

© *A.A. Tatarintsev, E.Yu. Zykova, A.E. Ieshkin, N.G. Orlikovsaya, E.I. Rau*

Moscow State University,
Moscow, Russia

E-mail: tatarintsev@physics.msu.ru

To establish the effect of subthreshold defect formation on the charge accumulation in quartz glasses, a comprehensive study of the process of their electrization by electron beams was carried out. Earlier it was shown that the process of radiative electrization of quartz glasses consists of two stages. The short-term stage of charging can be explained by the accumulation of charge on the initial trap centers, and the long-term component can be caused by the generation of deep trap centers capable of capturing electrons. In the studied quartz samples, the trapping centers can be three-coordinated silicon atoms (E'-centers). The presence of two stages of the charging process is confirmed by two different methods for determining the surface potential. Despite the increase in the surface potential during irradiation and the resulting decrease in the energy of the incident electrons, an increase in the intensity of the cathodoluminescent signal is observed. Such an increase in intensity can be caused by an increase in the number of luminescent defects in quartz, a two-coordinated silicon atom or a non-bridging oxygen atom, as well as by charge accumulation at competing nonradiative trap centers.

Keywords: radiation electrization of dielectrics, quartz glasses, charging under electron irradiation, radiation defect formation, dielectric charging kinetics.

1. Introduction

When dielectric materials are irradiated with electrons in their near-surface region, as a result of a number of self-consistent processes, an electric charge accumulates — radiation electrification of the dielectric. The study of the effects caused by radiation electrification is of fundamental scientific interest and of great practical importance. For example, radiation charging of the surface occurs during the operation of spacecraft, in nuclear power engineering, electron probe diagnostic research methods, electron beam lithography on dielectric substrates and in other fields.

In the nuclear power industry, promising matrices for the immobilization of radioactive waste from the nuclear fuel cycle are dielectrics (glass, ceramics). The process of their self-radiation inevitably leads to the accumulation of an electric charge, which leads to a Coulomb explosion or other phenomena that occur at high degrees of electrification of dielectric glasses [1].

The importance of understanding the charging processes of dielectrics for space exploration is associated with the development and creation of spacecraft and onboard scientific instruments (particle detectors, telescopes, spectrometers, communications equipment, etc.) resistant to aggressive factors of the space environment. According to space agencies, the main reason for the failure of geostationary satellites is the charging of dielectric components of spacecraft under the influence of electronic and ion radiation. As indicated in [2], in geostationary orbit, the total current of electrons to the spacecraft is about 1 nA/cm^2, and ions

(protons) 1 pA/cm^2. In this case, surface charging is usually caused by electrons with energy up to 50 keV, while internal charging occurs under the action of high-energy electrons $0.1-3$ MeV. In geostationary orbit, the average energy of plasma particles interacting with the spacecraft is several tens of keV. Thus, it is necessary to know the processes of electrification of materials by electrons and ions in the energy range from ~ 1 eV to 100 keV for increasing the operating time of the spacecraft and increasing the safety of manned space missions.

The effect of irradiation by charged particles on dielectrics has been studied for many years, but a number of aspects of this extremely complex phenomenon are still not fully understood and therefore require further clarification. The evolution of ideas about a complex self-consistent charging mechanism has progressed noticeably [3–5], but to date there is still no complete picture that holistically explains all the nuances of the processes of electronic charging of dielectric materials. As it was shown in the works of [6,7], the presence of electron traps, both initially existing in the crystal and created during electron irradiation due to the mechanisms of pre-threshold defect formation, has a significant effect on the process of radiation charging of dielectrics.

Due to the widespread use of silicon oxide, both crystalline (α-quartz) and amorphous (quartz glass), in various fields of engineering and technology, it has been studied quite intensively for many years. Many publications are devoted to the problems of electron probe charging SiO$_2$ targets studied with a scanning electron microscope [8–14].

But in all these publications, the question of the kinetics of charging SiO_2, about the time of the onset of the equilibrium state depending on the energy of the irradiating electrons, was not fully clarified. Ionizing radiation in optically transparent quartz glass can create various defects capable of capturing charge or generating luminescence, as well as post-emission of exoelectrons [15]. According to the energy position of the luminescence bands and their evolution depending on the dose of electron irradiation and temperature, we can expect new information about the nature of defects and other luminescence centers.

The purpose of the presented work was an experimental and theoretical study of the synergy of the charging process and the phenomenon of pre-threshold defect formation on the example of quartz glass. Quartz glass was chosen as a sample for the study, since the lattice defects in it are quite well studied. To establish the mutual influence of defect formation and the charging process, comprehensive studies of the evolution of the charging potential, integral luminescence, and cathodoluminescence spectra during its irradiation with electrons with an energy of $1-20\,keV$ were carried out.

2. Samples and experimental methods

The samples were quartz glasses with a purity of 99.99% with a size of $10 \times 10\,mm^2$ and a thickness of $1\,mm$ with the following parameters: permittivity $\varepsilon = 3.8$, electrical resistivity $\rho = 7 \cdot 10^7\,\Omega \cdot cm$. The band gap width of quartz glass is $E_g = 9\,eV$, which corresponds to the wavelength of $\lambda \approx 140\,nm$ of UV radiation during the transition of an electron from the conduction band to the valence band. It is worth noting here that the samples under study differ from other oxides and polymer dielectrics by significantly lower resistivity (by several orders of magnitude). In this regard, quartz glasses have a number of differences in their kinetic characteristics of charging as a function of the energy of irradiating electrons.

To prevent the influence of the electric field arising above the surface of the dielectric during charging on the electron beam, part of the samples was covered with a thin conductive gold film. The thickness of the film was selected so that the surface of the sample was still transparent to register cathodoluminescence, but at the same time the film had sufficient conductivity so that a charge could effectively flow through it onto a grounded substrate. The film was applied on the JEOL JFC-1100 cathode sputtering unit. The film thickness was measured on the chip of a silicon witness plate on a high-resolution scanning electron microscope and was $d \sim 10-14\,nm$. The areas of interaction of the electron beam with the initial quartz and with quartz coated with an Au film were calculated using the Casino v2.5 [16] program.

Studies of the dynamics of the surface potential of quartz during charging were carried out using an electrostatic electron spectrometer installed in a scanning electron microscope (SEM) LEO 1455VP [6]. In separate experiments

on the same SEM, an integral cathodoluminescence signal was recorded using the Centaurus detector in the range of visible wavelengths of $300-650\,nm$. Control experiments on X-ray microanalysis on SEM were carried out using the Oxford INCA X-act detector. In experimental processes, the irradiation of an area with the dimensions $100 \times 100\,mkm^2$ was carried out in the fast scanning mode with an electron beam with a current $I_0 = 1\,nA$. The pressure in the SEM chamber during cathodoluminescent and electron spectroscopic studies, as well as X-ray microanalysis, was about $\sim 5 \cdot 10^{-6}\,Torr$. The current was measured using a Faraday cylinder with a Keithley 6485 nanoammeter.

The cathodoluminescence spectra were recorded in Varian ultrahigh vacuum chamber using the Ocean STS-VIS microspectrometer in the wavelength range $350-850\,nm$. The base vacuum during the measurement of the cathodoluminescent signal was $10^{-8}\,Torr$ with oil-free pumping. The current density when registering the cathodoluminescent spectrum was $3 \cdot 10^{-3}\,A/cm^2$, a defocused beam with a diameter of $\sim 2\,mm$ was used for irradiation. Since the electron gun was limited to a maximum accelerating voltage of $3\,kV$, an additional potential was applied to the entire table on which the sample was fixed to accelerate the electrons to the required incident energy.

For the convenience of comparing experimental results obtained at different installations, all data are given in units of electron flux per cm^2.

3. Experimental results

Figure 1 shows the kinetics of changes in the integral cathodoluminescent signal and surface potential due to quartz charging when irradiated with an electron beam with an energy of $E_0 = 2.5, 5, 10$ and $15\,keV$ with a current density of $j_0 = 10^{-5}\,A/cm^2$. Cathodoluminescence signals were taken for two samples of quartz glass — the original sample and the Au film-coated one. In this case, the film was grounded to the substrate on which the sample was attached. During the experiment, the current from the sample substrate was monitored. In this case, there is no negative potential on the sample surface, and the actual electron energy will not decrease when approaching the sample surface. Since the cathodoluminescence signal on the samples with a film is significantly lower than for a pure sample, when registering the signal, it was necessary to change the gain of the recording PMT detector Centaurus. The data obtained were normalized to the maximum signal value for this sample obtained in the first $10\,s$ of recording for comparison of luminescent signals of different samples.

When quartz is electrified by an electron beam with an energy of $E_0 = 2.5\,keV$ and a current density of $j_0 = 10^{-5}\,A/cm^2$, the sample is not charged about $600\,s$, but then a rather slow charging occurs. A similar phenomenon during the exposure to electrons with an energy of 5 and $15\,keV$ was observed for sapphire in the papers [6,17]. For quartz glass, such a delay in the growth of the potential
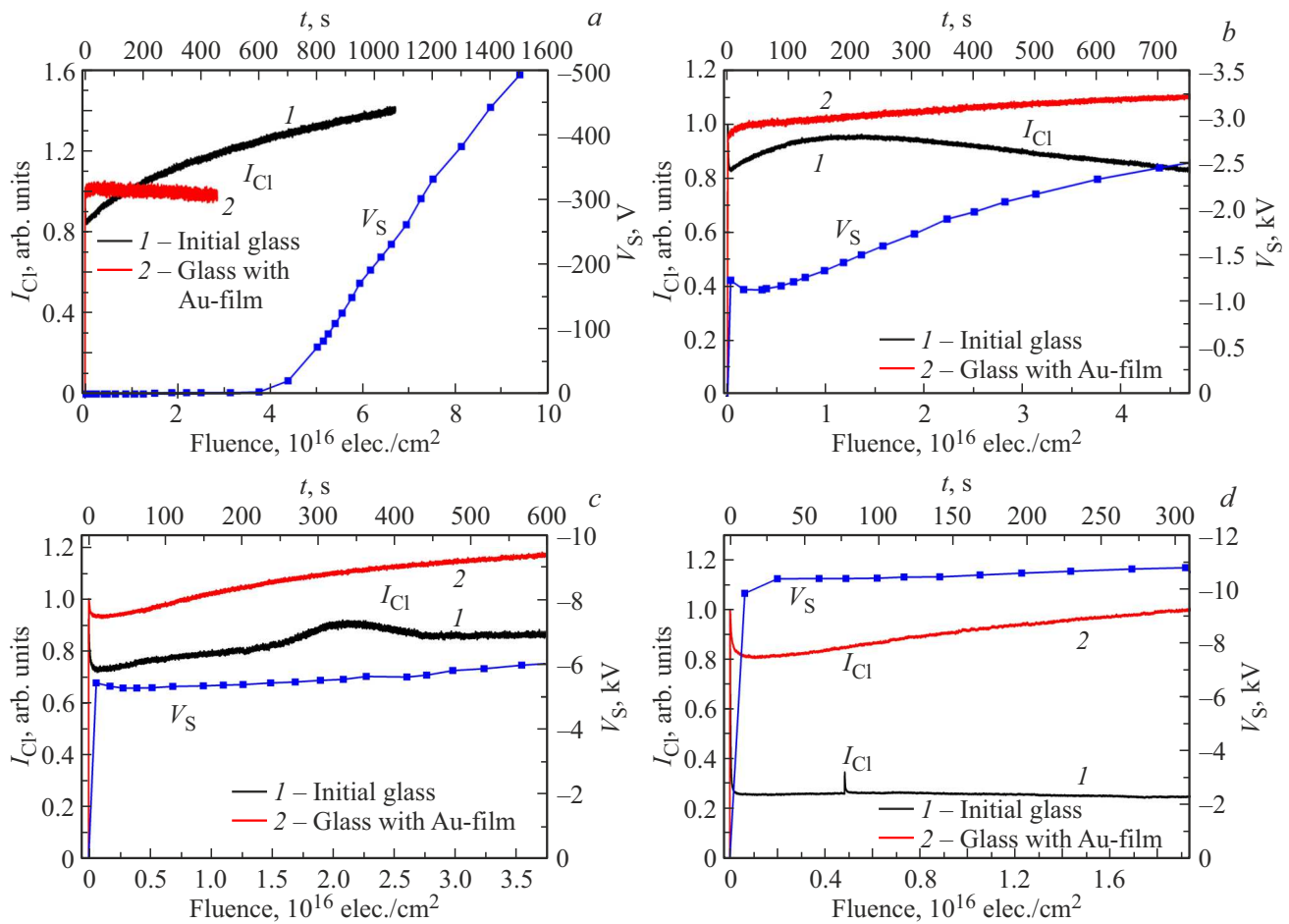
Figure 1. Dependence of ICL cathodoluminescence intensity and VS quartz charging potential on electron fluence, as well as on the irradiation time (upper scale) by electrons with energy $E_0 = 2.5$ (a), 5 (b), 10 (c) and 15 keV (d) current density $j_0 = 10^{-5}$ A/cm^2. The normalized dependences of the cathodoluminescence intensity on time are presented for the initial quartz (1) and the sample coated with an Au film with a thickness of 14 nm (2).

may be associated with the spreading of the charge over the surface due to the smallness of the resistance. Despite the fact that the actual energy of the electrons does not decrease, the cathodoluminescence signal for the original quartz not coated with a film increases. A slight change of the intensity of cathodoluminescence for a sample with a conductive film at a given energy of incident electrons is due to the fact that the main energy losses occur in the gold film. Figure 2 shows the results of numerical Monte Carlo simulation of electron trajectories for samples with and without Au film. The Casino v. 2.5 program used allows obtaining estimates of the energy loss region of primary electrons. Such estimates indicate that at the energy of primary electrons $E_0 = 2.5$ keV in such a film is absorbed up to 90% of the energy. At the same time, as the simulation shown in Fig. 2 shows, the primary electrons penetrate into the region under the film with sufficient energy to generate cathodoluminescence.

Let's estimate the current and energy of electrons passing through the film $d(\text{Au}) = 14$ nm. According to the work [18], the electron transmission coefficient through the

gold film is equal to

$$\eta_{\text{tr}} = \exp\left[-4.605\left(\frac{d}{R_0}\right)^{1.41}\right],$$

which gives for the gold film $d = 14$ nm, $\rho_m = 19.32$ g/cm^3, R_0 ($E_0 = 2.5$ keV) $= 90\rho_m^{-0.8}E_0^{1.3} = 27.7$ nm
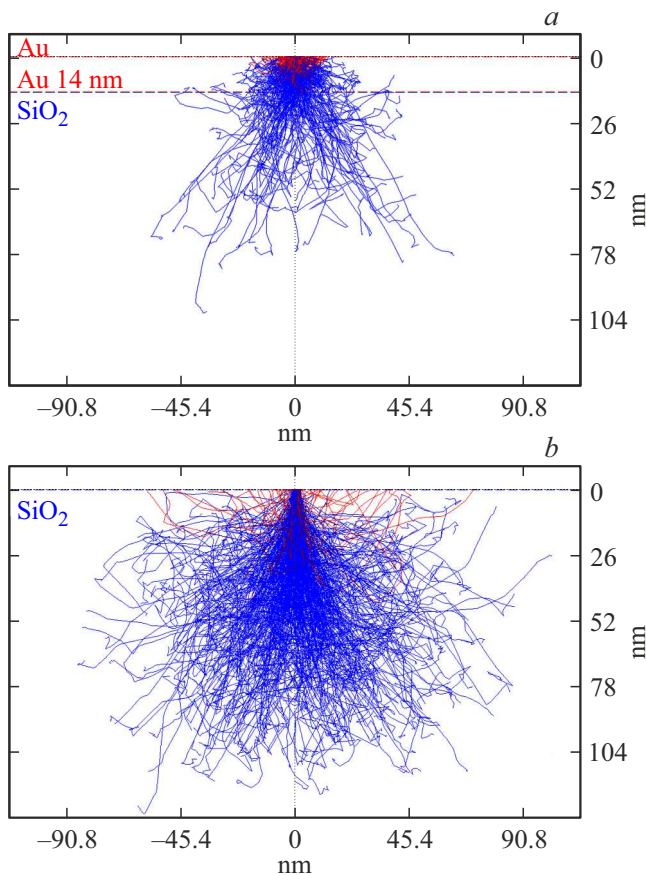
$$\eta_{\text{tr}} = \exp\left[-4.605\left(\frac{14}{27.7}\right)^{1.41}\right] = 0.172.$$

The average energy of the electrons passing through the gold film is determined by the coefficient ε_{tr}, which can be found from the following expression

$$\varepsilon_{\text{tr}} = C \times \exp\left[-\left(\frac{14}{27.7}\right)\right],$$

where

$$C = \frac{1 + 0.5\eta_0 + 0.5\eta_0^2}{1 + \eta_0} = 0.915 \quad (\text{for} \quad \eta_0(\text{Au}) = 0.45).$$

Figure 2. The interaction region of the electron beam with quartz glass at energy $E_0 = 2.5$ keV, coated with a film Au (*a*) and with the initial sample (*b*).

As a result, the coefficient is $\varepsilon_{\mathrm{tr}} = 0.552$, which means that 0.0952 of the initial beam energy, i.e. about 10%, will be absorbed in quartz glass under a gold film. In this case, the Au electrons passing through the film with energy $\langle E \rangle = \varepsilon_{\mathrm{tr}} \times 2.5 = 1.38$ keV will penetrate into SiO_2 ($\rho_m = 2.2$ g/cm^3) to a depth of ~ 73 nm, which corresponds to the calculations performed using the Monte Carlo method. Note that such energy is sufficient to generate a cathodoluminescent signal. It is to this depth that SiO_2 is charged under the influence of a weakened electron beam with energy 1.38 keV, i.e. in this situation SiO_2 is practically not charged. These considerations can also be carried out on the energy $E_0 = 5, 10, 15$ keV.

For high values of the electron beam energy, quartz glass, despite the relatively low resistance, is rapidly charged at the initial moment of time. In our experiments, at $E_0 = 5$ keV (Fig. 1, *b*), the sample is charged in less than 4 s negatively to the value of $V_S \simeq 1.2$ kV, while the actual energy of the irradiating the number of electrons decreases to the value $E_L = 3.8$ keV. At the same time, the integral cathodoluminescent signal decreases by $\sim 20\%$, which is caused by a decrease in the cathodoluminescent signal generation region with a decrease in the actual incident

energy. Further, the cathodoluminescence signal begins to grow significantly over the next $60-80$ s, with the surface potential unchanged. Such an increase may be associated with an increase in the number of defects, which are the centers of luminescence, in the material during electron irradiation. After some time, the absolute value of the surface potential begins to increase, which leads to the maximum of the cathodoluminescent signal, and then its decline.

If the surface of the sample is covered with a thin conductive film through which the charge can flow to the ground, then the energy of the incident electron beam will not change until it enters the dielectric. Consequently, if there are no significant internal fields, then the cathodoluminescence output region will practically not decrease. As can be seen from Fig. 1, *b*, the intensity of the cathodoluminescent signal of quartz with a grounded film increases almost linearly with the irradiation time. Possible reasons for such an increase in the cathodoluminescence signal will be discussed in the next section. At the same time, such changes in the intensity of the cathodoluminescence signal, as on a sample without a film, are not observed.

For the energy of the charging electron beam $E_0 = 10$ and 15 keV, a rapid increase in the surface potential is also observed (Fig. 1, *c* and *d*). At the same time, the cathodoluminescence intensity decreases synchronously at the initial moment of time: for $E_0 = 10$ keV, such a decrease occurs by $\sim 30\%$, and for 15 keV by $\sim 75\%$. For $E_0 = 10$ keV, the first spectrum registered after 10 s, indicates charging of the surface to $V_S = -5.4$ kV. A the equilibrium state of the surface potential $V_{S0} = -7.1$ kV is reached in 1500 s. It also shows two stages of establishing the equilibrium charging potential [6]: short-term — in units of seconds and long-term — in hundreds of seconds. As can be seen from Fig. 1, *d*, a similar two-stage process of establishing the dynamic equilibrium of the surface potential is observed in case of exposure to electron beams with energy of $E_0 = 15$ keV. For the first 10 s potential V_S reaches -9.8 kV, and for a longer time ~ 300 s equilibrium value -10.8 kV. A similar monotonous increase of cathodoluminescence intensity is observed for these energies on quartz glass samples coated with a conductive film after the initial decline. Such an initial decrease in the intensity of cathodoluminescence can be explained by a decrease in the volume of generation of the luminescence signal due to the inhibition of the electron beam by an internal field in quartz under a conductive film. In this case, the conductive film shields the charging potential for the primary beam, but if a negative electric charge accumulates inside the quartz at depths of the order of $1-2\,\mu$m, then a field will arise under the film in the dielectric that inhibits the primary electron beam. This means that the cathodoluminescence area will shrink, causing a reduction of the radiation intensity. Further monotonous growth may be caused by the generation of new radiative recombination centers.

The method of determining the surface potential from the spectra of secondary electrons can be sensitive to
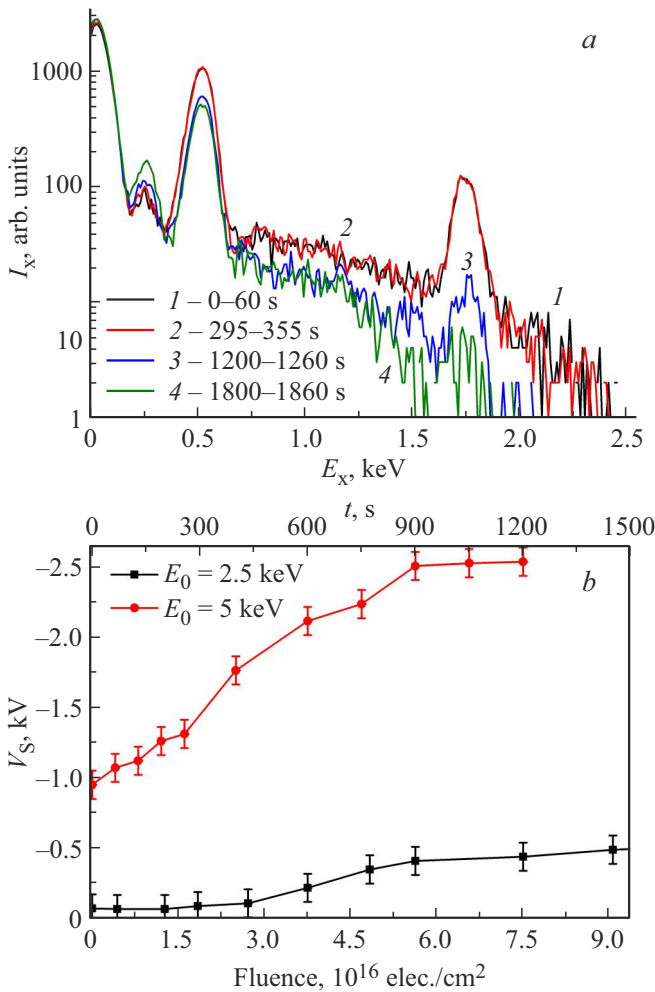
Figure 3. (*a*) X-ray spectra during quartz charging at the energy of incident electrons $E_0 = 2.5$ keV. Spectrum collection times: *1* — spectrum registered during 60 s, *2* — the beginning of spectrum accumulation after 295 s from the start of charging, *3* — after 1200 s, *4* — after 1800 s. (*b*) The potential of the quartz surface obtained from the position of the high-energy boundary of the braking X-ray spectrum during charging quartz with electrons with energy $E_0 = 2.5$ and 5 keV. Current density $j_0 = 10^{-5}$ A/cm^2. Spectrum accumulation time 60 s.

local inhomogeneities of the field above the surface of the charging sample. An experiment was conducted to measure the surface charging potential by shifting the braking boundary of the X-ray spectrum to confirm the fact that quartz is not charged at the initial moment of time when irradiated with electrons with an energy of $E_0 = 2.5$ keV. The accumulation time of the spectrum $50-60$ s will be enough to qualitatively trace the charging trend and confirm the characteristics presented above since quartz is not charged in the first 600 s (see Fig. 1). It is worth noting here that there is a large error in detecting the braking boundary due to the small number of high-energy quanta. In addition, the accumulation time of the X-ray spectrum was quite long (60 s), which also introduces its own uncertainty

in determining the position of the spectrum boundary in time. The data of the X-ray spectrum measurement results are shown in Fig. 3, where the spectra of the braking X-ray radiation for the energy of the electron beam $E_0 = 2.5$ keV, as well as the time dependence of the charging potential obtained from the position of the high-energy boundary for two values of the energy of the primary beam $E_0 = 2.5$ and 5 keV. These data are qualitatively consistent in time with the data presented in Fig. 1 and confirm the delay in the accumulation of potential.

The analysis of the kinetic characteristics of the charging potential $V_s(t)$, presented in Fig. 1, shows a striking difference between $V_S(t)$ at $E_0 = 2.5$ keV from the case of charging at $E_0 = 5, 10$ keV. To clarify the reasons for this difference, additional experiments were carried out to register kinetic characteristics by detecting secondary and reflected electrons using a standard backscattered electron detector in SEM. This method is described in detail in our work [19]. The dependence of the total emission current I_σ and the current from the sample holder I_{L+D} on the irradiation time was also measured. The results of experimental measurements at $E_0 = 2.5$ and 10 keV are shown in Fig. 4, *a, b*. These figures show calibration signals taken on a massive sample of Al at electron probe currents $I_0 = 1$ and 5 nA for both energies of incident electrons.

Fig. 4, *a* shows the dependences of the signal from the reflected electron detector for quartz glass I_{SiO_2}, as well as the current from the sample holder I_{L+D} when the sample is irradiated with electrons with an energy of 10 keV. Based on the kinetic characteristics of the current I_{L+D}, which is the total leakage and displacement current, and the signal from the reflected electron detector, it follows that the time to establish the equilibrium potential is $\tau_0 \approx 30-40$ s. At the same time, at $E_0 = 2.5$ keV, the equilibrium state for the characteristics presented in Fig. 4, *b* occurs approximately in the same time. At the same time, the value of the signal from the reflected electron detector for $E_0 = 2.5$ keV signal is lower than the calibration value of the signal from aluminum at the same energy, although at high energy ($E_0 = 10$ keV) the signal is higher than the signal from aluminum at ~ 4 times. This difference is caused by the contribution of accelerated secondary electrons to the signal at the energy $E_0 = 2.5$ keV [19]. The reason for the differences is that, SiO$_2$ is initially charged positively. Indeed, for SiO$_2$, the maximum value of the secondary electron emission coefficient is $\delta = 3.5$ at $E_{0m} = 0.5$ keV, and the energy for an uncharged sample is $E_{02} = 4$ keV at which the total emission coefficient is $\sigma = 1$. Therefore, with the taken energy $E_0 = 2.5$ keV $\sigma > 1$, the sample is positively charged in units or fractions of volts. In this case, the current from the sample should be positive, but this current is negative in Fig. 4. This suggests that the leakage current I_L, and not the bias current I_d, makes the dominant contribution to the value of the current from the sample, this weak positive potential is not fixed in our experiments. But as the radiation dose increases, pre-threshold free electron capture centers are formed in the
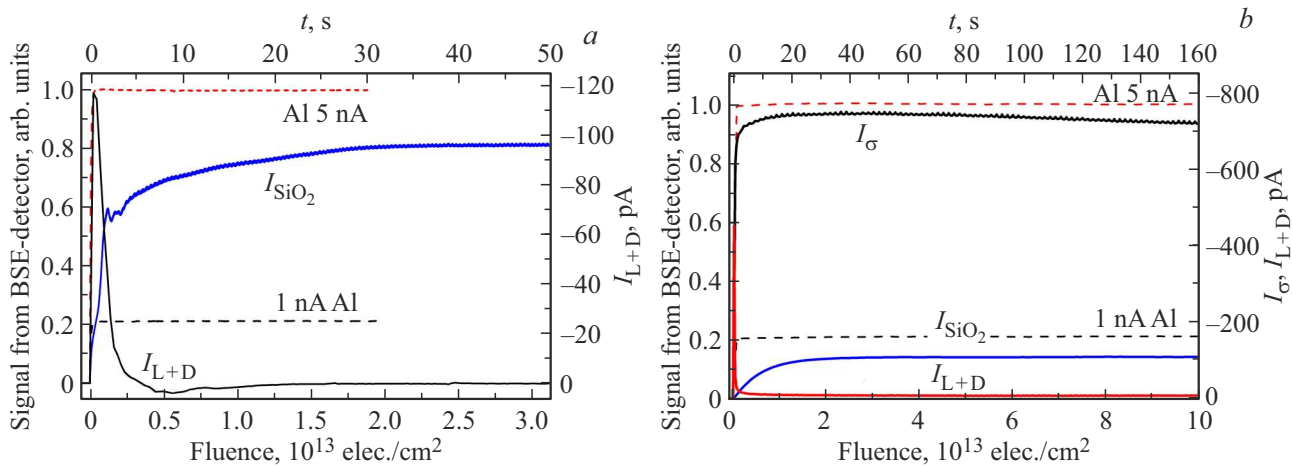
Figure 4. Dependence of the signal from the reflected electron detector I_{SiO_2} and current characteristics on the electron fluence and on the irradiation time (upper scale) by electrons with energy 10 (*a*) and 2.5 keV (*b*). Dashed lines in the figure represent calibration signals from Al at a current of 1 and 5 nA.

region of $R_0 > 20$ nm and the sample begins to slowly charge negatively (Fig. 1, *a*). This process is long-term, as it affects the rather high conductivity of SiO_2 quartz glass. The leakage current can be estimated by the formula $\rho_r = \frac{V_s a^2}{I_L d}$, where ρ_r — resistivity, a — side of the irradiated area (cm), d — thickness of the sample. In our case $+V_S = 1$ V, $d = 1$ mm, $a = 1$ mm should be $I_L = 10^{-9}$ A, which is not observed. Consequently, the electrons from the irradiation zone do not reach the sample substrate, but spread throughout the sample, forming a weak bulk density of negative charges. Over time, as deep radiation centers are formed, the resistivity at the irradiation site increases by orders of magnitude, and, consequently, I_L tends to zero, and $-V_S$ slowly increases, which is confirmed by the characteristic of $V_S(t)$ in Fig. 1, *a*. It is possible that the processes considered are accelerated many times already at the initial moments of irradiation at the energy $E_0 = 5$ keV and more.

4. Discussion of results

Cathodoluminescent spectra were collected at the energy of incident electron beams with energies $E_0 = 5$ and 15 keV to understand the structural changes in quartz glasses during charging. Figure 5 shows the cathodoluminescence spectra of quartz glass depending on the time of irradiation with electrons with energy $E_0 = 5$ keV. In the quartz cathodoluminescence spectrum, two main luminescence bands are observed, having intensity maxima at an energy of 2.7eV (wavelength 460 nm) and 1.9eV (650 nm), which can be interpreted as the emission of intrinsic defects.

Indeed, the position of the line we observed at an energy of 1.9 eV (wavelength 650 nm) in accordance with the literature data [20,21] is associated with the radiation of the hole center of the non-bridge oxygen atom ($\equiv$ **Si**−**O**$^-$). A non-bridged oxygen atom is one of the defects of a

complementary pair of elementary intrinsic defects of a quartz crystal formed as a result of the rupture of the silicon-oxygen bond. The second defect of this pair — a three-coordinated silicon atom can be transformed into a two-coordinated silicon atom (=**Si**:), characterized by two luminescence bands with energies 2.7 eV and 4.4 eV [20–22] as a result of interaction with incident electrons. At the same time, the three-coordinated silicon — the so-called E'-center is a well-studied paramagnetic non-luminescent center.

Such defects are caused by broken bonds when the orbitals of neighboring atoms do not overlap due to the displacement of oxygen and silicon atoms over such a distance that the bond length **Si**−**O**−**Si** becomes greater than 3.2 eV, i.e. the bond between adjacent tetrahedra is destroyed. At the same time, an electron can be captured on a free silicon bond, and an oxygen — hole [23]. An energy exceeding the energy of the chemical bond is required to break a regular network of quartz glass bonds and amounts to approximately 8−9 eV, which is significantly less than the energy required for the formation of defects during elastic interaction.

An increase in the intensity of cathodoluminescence lines is observed during electron beam irradiation (Fig. 6) associated with a non-bridged oxygen atom (1.9 eV) and with a two-coordinated silicon atom (2.7 eV). A similar increase in luminescence intensity under electron irradiation was first detected in yttrium-aluminum garnet doped with neodymium in the work [24]. It is indicated in that paper that the growth of the cathodoluminescence signal may be associated with the filling of competing nonradiative centers. Indeed, as the non-radiative centers fill up, more and more electrons will participate in radiative recombination, which will lead to an increase in the intensity of the cathodoluminescent signal. The capture of electrons by nonradiative traps should lead to the accumulation of charge and, as a consequence, an increase in the surface potential.
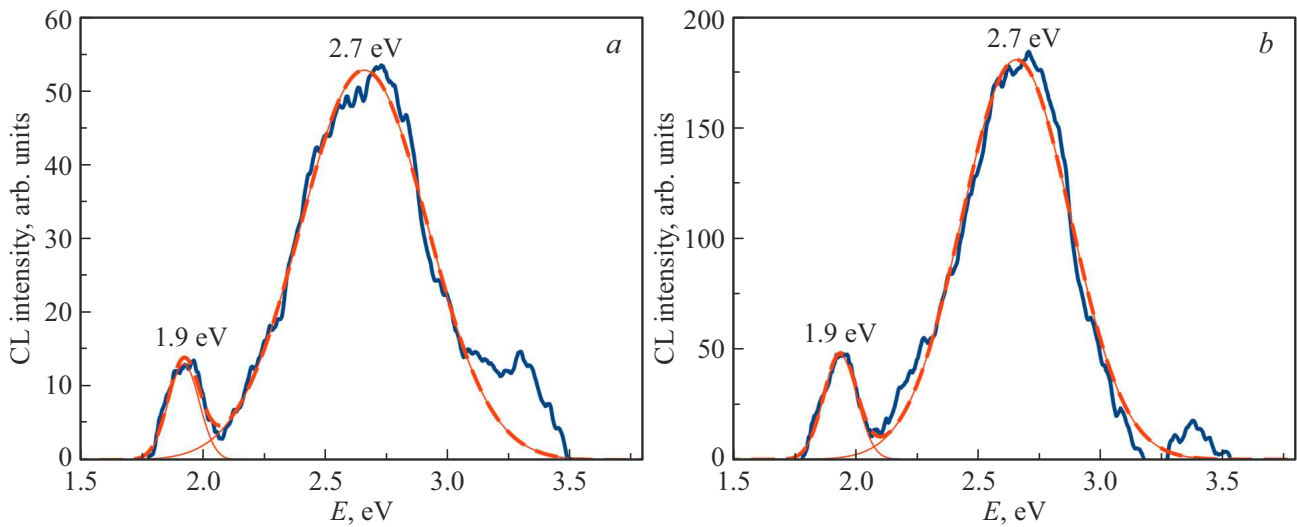
Figure 5. Cathodoluminescence spectra of quartz glass under a gold film 11 s after the start of irradiation (*1*) and 530 s (*2*). The spectra were taken at $E_0 = 5$ keV.
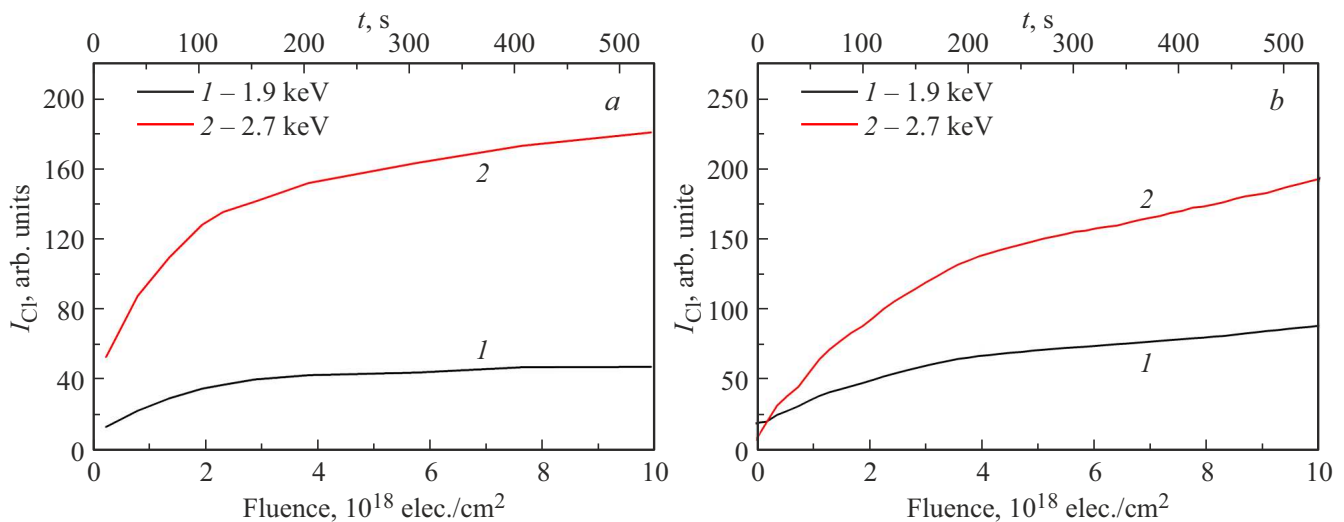
Figure 6. Dynamics of the intensity of cathodoluminescence lines associated with a non-bridge oxygen atom (line *1*) and with a two-coordinated silicon atom (line *2*) from the electron fluence (irradiation time) for the primary beam energy $E_0 = 5$ and 15 keV. Current density $j \sim 3 \cdot 10^{-3}$ A/cm^2.

However, as our experiments show (see Fig. 1), even with a slight increase in the surface potential, there is an increase in both the integral signal of cathodoluminescence and cathodoluminescent lines associated with non-bridge oxygen (line 1.9 eV) and a two-coordinated silicon atom (2.7 eV). Such an increase in cathodoluminescence intensities with a noticeable slowdown in the growth of the surface potential (for 5 keV, it does not change about $60-80$ s) can be explained by an increase in the number of luminescent centers. An increase of the intensity of cathodoluminescence indicates an increase in defects of such as luminescent centers, and a corresponding increase in complementary defects, i.e. deep defects capable of capturing electrons. Such defects may include the E'-center,

and the accumulation of electrons on such centers leads to a further increase in the potential of the surface — i.e., to the charging process.

Also a memory effect in yttrium aluminum garnet doped with neodymium was observed in paper work [24], i.e. the intensity of cathodoluminescence of the region previously irradiated with electrons, noticeably exceeded the intensity of the previously unirradiated region during repeated irradiation. At the same time, such a memory effect persisted for a long time as it was noted in this study. A similar memory effect of cathodoluminescence intensity was observed in quartz in our experiments. Most likely, a combination of both of these mechanisms of enhancement of the intensity of luminescence is possible

in case of radiation electrification of quartz. Along with the accumulation of charge on competing non-radiative trap centers, the formation of additional radiative defects (a two-coordinated silicon atom and a non-bridged oxygen atom) and complementary non-radiative defects (E'-centers) is possible, as evidenced by the long-term stage of the quartz charging process under electron irradiation.

5. Conclusion

The process of radiation electrification of quartz glasses consists of two stages. Short-term charging stage — the sample is charged to a high potential value in units of seconds, which can be explained by the accumulation of charge on the initial trap centers contained in quartz. The long-term component following it may be caused by the generation of electron capture trap centers. In the quartz samples under study, such capture centers may be three-coordinated silicon atoms (E'-center).

The presence of two stages of the charging process is confirmed by two different methods for determining the surface potential — by electron spectrometry and by shifting the high-energy braking boundary of X-ray radiation, as well as by registering reflected electrons together with accelerated secondary electrons from the dielectric during charging. At the same time, the slowdown in the growth of the surface potential for low values of incident energy ($E_0 \leq 5 \, \text{keV}$) can be explained by positive charging of the surface or spreading of the charge due to the relatively small resistance of quartz glasses. Further accumulation of charges will take place when electrons are captured on newly created relatively deep traps.

The intensity of the cathodoluminescent signal mainly increases despite the increase of the surface potential and the decrease of incident energy caused by it. Such an increase of intensity can be caused by an increase of the number of luminescent defects in quartz which is a two-coordinated silicon atom or a non-bridged oxygen atom, which confirms the growth of the cathodoluminescent signal with a decrease in the rate of accumulation of the surface potential. In some cases, the mechanism of growth of the cathodoluminescent signal due to the accumulation of charge on competing non-radiative trap centers is also possible.

Funding

Conflict of interest

The authors declare that they have no conflict of interest.

References

[1] M.I. Ojovan, B.E. Burakov, W.E. Lee. J. Nucl. Mater. **501**, 162 (2018).

[2] L.S. Novikov. Radiation effects on spacecraft materials. University book, M. (2010). 192 p. (in Russian).

[3] J. Cazaux. J. Appl. Phys. **89**, 8265 (2001).

[4] A. Melchinger, S. Hofmann. J. Appl. Phys. **78**, 6224 (1995).

[5] N. Cornet, D. Goeuriot, C. Guerret-Piecourt, D. Juve, D. Treheux, M. Touzin, H.-J. Fitting. J. Appl. Phys. **103**, 064110 (2008).

[6] E.I. Rau, A.A. Tatarintsev. Phys. Solid State **63**, *4*, 574 (2021).

[7] E.I. Rau, A.A. Tatarintsev. J. Appl. Phys. **132**, 184102 (2022). doi.org/10.1063/5.0104628

[8] J.P. Vigouroux, J.P. Duraud, A. Le Moel, C. Le Gressus, D.L. Griscom. J. Appl. Phys. **57**, *12*, 5139 (1985). DOI: 10.1063/1.335247.

[9] K.H. Oh, C.K. Ong, B.T.G. Tan, G. Le Gressus. J. Appl. Phys. **74**, *11*, 6859 (1993). DOI: 10.1063/1.355087.

[10] H. Gong, C.K. Ong. J. Appl. Phys. **75**, *11*, 449 (1994). DOI: 10.1063/1.355873.

[11] K.H. Oh, C. Le Gressus, H. Gong, C.K. Ong, B.T.G. Tan, X.Z. Ding. J. Appl. Phys. **74**, *2*, 1250 (1993). DOI: 10.1063/1.354928.

[12] B. Askri, K. Raouadi, R. Renoud, B. Yangui. J. Electrostat. **67**, 695 (2009). DOI: 10.1016/j.elstat.2009.03.006.

[13] S. Fakhfakh, O. Jbara, S. Rondot, A. Hadjadj, J.M. Patat, Z. Fakhfakh. J. Appl. Phys. **108**, 093705 (2010). DOI: 10.1063/1.3499692.

[14] S. Fakhfakh, O. Jbara, M. Belhaj, Z. Fakhfakh, A. Kallel, E.I. Rau. Eur. Phys. J. Appl. Phys. **21**, 137 (2003). DOI: 10.1051/epjap.

[15] H.-J. Fitting, T. Barfels, A. von Czarnowski, A.N. Trukhin. Mater. Sci. Eng. B **71**, 109 (2000).

[16] D. Drouin, A.R. Couture, D. Joly, X. Tastet, V. Aimez, R. Gauvin. Scanning **29**, 92 (2007).

[17] E.I. Rau, A.A. Tatarintsev, V.V. Khvostov, V.E. Yurasova. Vacuum **129**, 142 (2016).

[18] H.J. Fitting. J. Electr. Spectr. Rel. Phemom. **136**, *3*, 265 (2004). DOI: 10.1016/j.elspec.2004.04.003

[19] S.V. Zaitsev, E.Yu. Zykova, E.I. Rau, A.A. Tatarintsev, V.A. Kiselevsky. PTE **6** (2023). (in Russian).

[20] L. Skuja. J. Non-Cryst. Solids **239**, 16 (1998).

[21] H.-J. Fitting, T. Barfels, A.N. Trukhin, B. Schmidt. J. Non-Cryst. Solids **279**, 51 (2001).

[22] L. Skuja, N. Ollier, K. Kajihara. Rad. Measurements **135**, 106373 (2020).

[23] B. Balland. „Defects in silica films" in „Instabilities in silicone devices"/ Ed. G. Barbottin, A. Vapaille. North-Holland. (1986). P. 101–153.

[24] K.N. Orekhova, A.N. Trofimov, M.V. Zamoryanskaya, V. Strenk. Optika i spektroskopiya **120**, *6*, 956 (2016). (in Russian).

Translated by A.Akhtyamov